Protein & Cell

REVIEW

Protein microarray biosensors based on imaging ellipsometry techniques and their applications

Yu Niu[1,2], Gang Jin[1] ✉

[1] NML, Institute of Mechanics, Chinese Academy of Sciences, Beijing 100190, China
[2] Graduate School of the Chinese Academy of Sciences, Beijing 100049, China
✉ Correspondence: gajin@imech.ac.cn
Received March 24, 2011   Accepted May 12, 2011

ABSTRACT

After years of development, biosensors based on imaging ellipsometry and biosensors based on total internal reflection imaging ellipsometry have been successfully implemented in various engineering systems. Their experimental setups, detection principles, and biological and clinical applications are briefly reviewed.

KEYWORDS   biosensor, protein microarray, imaging ellipsometry, total internal reflection imaging ellipsometry, applications

INTRODUCTION

After the completion of the Human Genome Project, proteomics entered the spotlight of biological research. Proteomics has increasingly drawn attention from simply identifying novel genes to determining the functions of the proteins that they encode. Similar to genome research, studying the characteristics of protein-protein interactions requires the ability to perform massively parallel analyses (Yu et al., 2006). Microarray technology is a promising method to provide an effective solution for simultaneous detection of various analytes in a single experiment (Bally et al., 2006). Microarrays are built by assembling a set of ligands onto a solid surface and are suitable for high-throughput analyses. Compared to traditional immunological methods, protein microarrays have several distinct advantages (Rich and Myszka, 2007; Klenkar and Liedberg, 2008), including low consumption of both the ligand and analyte, parallel screening of multiple interactions, and rapid response readout. Based on diverse detection technologies, protein micro-

arrays can form the basis of various types of biosensors as the ideal analytical tools for proteomics (Templin et al., 2003).

Biosensors fall into two categories: labeled and label-free biosensors. Commonly used labels include fluorescent dyes (Ligler et al., 2003), enzymes (Engvall and Perlmann, 1971), radioactive labels (Aicher et al., 2003), and the more recently developed quantum dot (Chan and Nie, 1998). They provide ultra-high throughput readout of protein-protein interactions with good detection sensitivity, specificity, and reliability. Many of the commercially available protein microarray biosensors are labeled (Bally et al., 2006; Boozer et al., 2006). However, such arrays have several drawbacks (Kodadek, 2001). First, labeling may change protein conformations and impair bioactivity. This can be especially severe for low molecular weight proteins and peptides with only a few epitopes. Second, labeling may result in difficulties in quantification. In addition, the labeling process is normally time and labor intensive. To solve these problems, substantial effort has been devoted to the development of label-free protein biosensors, though their detection sensitivity for certain biomolecules is lower than that of labeled biosensors (Anastasiadou et al., 2008).

Detection of interactions with label-free biosensors relies on acoustic methods, notably surface plasmon resonance (SPR) (Hutter and Fendler, 2004), imaging ellipsometry (Jin et al., 1995), revamping calorimetry (Ladbury and Chowdhry, 1996), quartz crystal resonators (Lucklum and Hauptmann, 2000), nanowires (Wanekaya et al., 2006), and ion channel switch technology (Cornell et al., 1997). Currently, SPR biosensors play a dominant role because they have been intensively developed for commercial applications in the last 10 years.

SPR is a label-free detection method for analyzing

biomolecular interactions in real-time (Jain et al., 2007). By replacing photonic detectors with CCD cameras, SPR imaging (SPRi) improves the throughput of conventional SPR to analyze multiple interactions in parallel. SPRi offers the possibility to simultaneously monitor hundreds of biological interactions and estimate the kinetic parameters of the interactions between the ligands immobilized on the biosensor surface and analytes in solution (Scarano et al., 2010; Kodoyianni, 2011). Thus far, SPRi has been used for a wide range of biological applications (Campbell and Kim, 2007), varying from hybridization reactions with DNA to protein–protein interactions. However, to date, little has been done to apply SPRi in commercial practices, such as clinical diagnostics, food analysis, and pharmaceutical research (Kodoyianni, 2011).

Ellipsometry is a conventional optical technique for measuring changes in light polarization states, and it can determine film thickness with a resolution of ⩽ 0.01 nm as a nondestructive and label-free method (Arwin, 1998). Imaging ellipsometry is an enhancement of standard single beam ellipsometry that combines the power of ellipsometry with microscopy (Jin, 2008). A high spatial resolution, on the order of micrometers (laterally) and sub-nanometers (vertically), can be achieved with a large viewable area (several square centimeters), which allows simultaneous multi-sensing of target microarrays.

The concept of biosensors based on imaging ellipsometry (BIEs) was proposed in 1995 for the visualization of biomolecular interactions (Jin et al., 1995, 1996). Over the past 16 years, commercial products based on single wavelength and spectroscopic imaging ellipsometry, made by the Nanofilm Company (http://www.nanofilm.de/; Gedig et al., 2008), have entered the market, and many significant improvements (e.g., the off-null sampling method (Chen et al., 2007a), spectroscopic technique (Meng and Jin, 2011), automatic control, microarray surface modification (Wang and Jin, 2003a, 2004a, b), micro-fluidic reactors (Jin and Wang, 2002; Wang et al., 2006), bio-system optimization, and protein interaction databases) have been introduced into BIE to improve its performance and feasibility. Therefore, BIE has been developed into an automatic device for quantitative and high-throughput protein analysis (Jin et al., 2011). BIE's sensitivity is on the order of 1 ng/mL for immunoglobulin G detection without any labeling (Jin, 2008; Qi et al., 2009b). Thus far, BIE has successfully been used in a wide range of biomedical and clinical detection applications (Qi et al., 2009a, 2009b, 2010; Huang et al., 2011).

In recent years, biosensors based on total internal reflection imaging ellipsometry (BTIRIEs) (Chen et al., 2007b) have been developed to meet the need of kinetic process analysis of biomolecular interactions. In BTIRIE systems, imaging ellipsometry is performed in the total internal reflection mode, and the change of the evanescent wave field near the sensing surface is used to describe the biomolecular interactions. BTIRIE offers a much higher sensitivity because of its phase-sensitive property (Liu et al., 2011). Theoretically, BTIRIEs are 30 times more sensitive than the conventional SPR method (Asinovski et al., 2008) after optimization, including polarization setting, the spectroscopic technique, and the use of a cooled imaging device to improve the signal-noise ratio and detection limit (Liu et al., 2010, 2011).

In this review, the working principles, experimental approaches, and biomedical applications of two types of biosensors based on imaging ellipsometry are summarized.

BIEs

Generally, a BIE system can be divided into four parts: the microarray reactor, the imaging ellipsometer, the control system, and the biosensor database, as shown in Fig. 1 (Jin, 2008). The microarray reactor serves to fabricate the protein microarray and accommodate biomolecular interactions. Using the micro-fluidic reactor, various ligands are delivered to different cells to form a sensing array, and each sensing surface can be prepared homogeneously under the flow condition. The imaging ellipsometer acts as a reader for data acquisition from the microarray. Imaging ellipsometry is an enhancement of standard ellipsometry, which combines the power of ellipsometry with microscopy (Jin et al., 1995, 1996). The latest imaging ellipsometer is a spectroscopic imaging ellipsometry (SIE) system (Meng and Jin, 2011). Compared to single-beam imaging ellipsometers, SIEs have advantages in achieving the thickness distribution on a solid substrate with optical lateral resolution on the order of microns upon magnification (Meng and Jin, 2011). SIEs can be used to visualize ultra-thin films and the concentration change of a molecular mass surface (Jin et al., 1995, 1996). Slight variations of thickness can be remarkably distinguished by imaging ellipsometry, and the results are represented as grayscale images (Jin, 2008). The grayscale value is approximately linearly proportional to the thickness of the molecular film (Chen et al., 2007a). The control system is responsible for combining the microarray reactor with the imaging ellipsometer and functions to control the hardware's mechanical motion and obtain results in images. Indeed, the control system is the central piece of an automated biosensor. The biosensor database is used to aid BIE users in determining optimized experimental conditions by comparing previously stored data to current requirements.
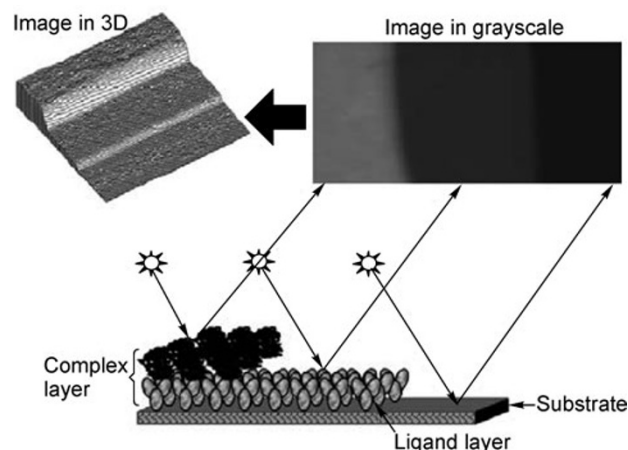
BIE DETECTION PRINCIPLE AND PROCEDURES

BIEs are used to visualize the thickness distribution of protein layers attached to a patterned surface on a solid substrate, as shown in Fig. 2 (Jin, 2008). A ligand and its receptor (e.g., an antibody and its corresponding antigen, respectively) can assemble into bio-complexes due to their affinity. The optical
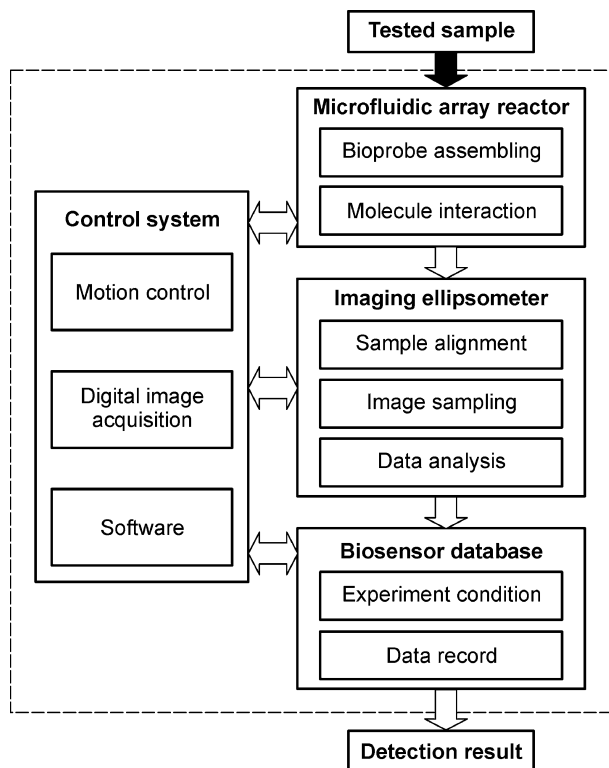
Figure 1. Schematic diagram of BIE. The solid arrow indicates the physical flow of a sample; the empty arrows indicate the data flow (Jin, 2008).

Figure 2. BIE detection principle. The incident wave of the polarized light as probe beam irradiates the sample and the reflective beam carries sample information, such as surface concentration of the immobilized protein molecules. The three parts of the sample, including bear substrate, ligand layer and complex layer, can be differentiated in the ellipsometric image that reveals different reflection intensities in grayscale. Surface concentration distribution of the protein layer can be further demonstrated in a 3D plot (Jin, 2008).

biosensor is based on the fact that each reactant, such as a ligand, is immobilized to a surface to form a monolayer, acting as a bioprobe via its bioactivity. The other reactant, such as the analyte (or receptor), exists in a solution. The bioprobe is then exposed to the solution containing the analyte. When the analyte in the solution interacts with its corresponding ligand, they assemble into a complex based upon their inherent binding affinity. The molecular mass surface concentration where the interaction takes place becomes higher than before exposure to the analyte solution. A significant increase of the surface concentration indicates that the solution contains the receptor bound to the ligand. With the visualization of imaging ellipsometry, which has high vertical and lateral spatial resolution (on the order of 0.1 nm and 1 μm, respectively), the increase in surface concentration can be determined, and in this way, the existence of the analyte in the solution is verified. Many bioprobes can be arranged in a matrix to form a protein microarray for multi-detection (Jin and Wang, 2002; Wang and Jin, 2003b).

The general detection procedure with BIEs can be summarized with the following successive steps. First, the substrate is modified with chemical reagents to attach to a chemically modified surface. Then, the modified surface is placed in the micro-fluidic reactor system to form patterned cells in an array format. Different ligand solutions are separately pumped into each cell to immobilize ligand on the microarray. Following this, the analyte solution is delivered to react with the ligands. Finally, the microarray is sampled by the imaging ellipsometry reader to determine molecular interaction results.

BIE BIOMEDICAL AND CLINICAL APPLICATIONS

BIEs are usually set to work in the *ex-situ* mode, which is suitable for most clinical detection applications (Jin et al., 2011). Thus far, BIEs have successfully been used in a wide range of biomedical and clinical detection applications. Here, some typical applications are presented.

Antibody screening

Antibody screening is an important process in a wide range of biomedical and clinical applications. Niu et al. (2011) employed a BIE as an antibody screening platform to compare and evaluate five ricin antibodies (named 7G7, pVHHS1, 5S1R, VHHS1, and S1R). Ricin, whose estimated oral lethal dose is < 20 mg/kg body weight in humans, is one of the most potent plant toxins known. Antibodies against ricin can identify and neutralize the toxin quickly and efficiently and are thus of great significance for the diagnosis and treatment of patients exposed to ricin poison. All five antibodies react with 50 μg/mL ricin but not abrin, a ricin analog (Fig. 3A). When the ricin concentration was decreased to 1 ng/mL, the limit of detection (LOD) values of 7G7, pVHHS1, 5S1R,
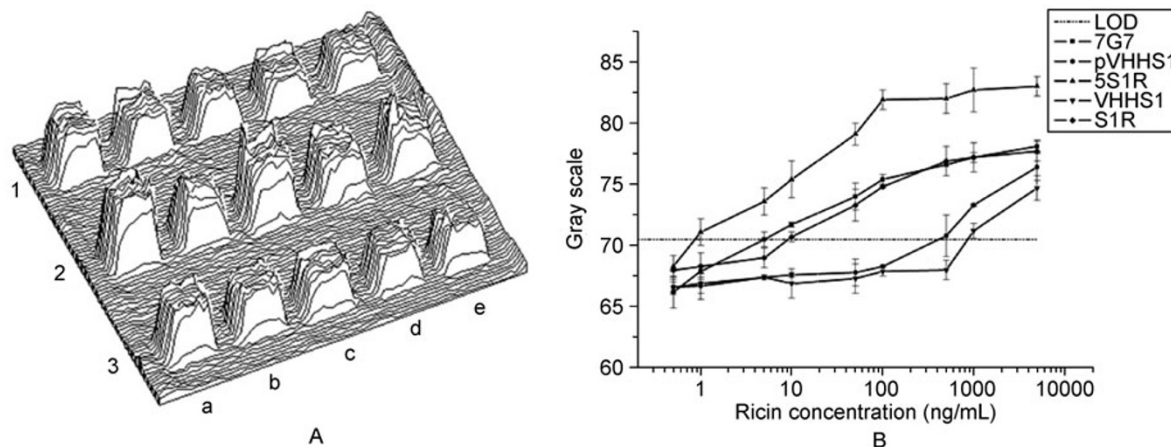
Figure 3. Ricin detection with BIE. (A) 3D image of the interaction between ricin and its five antibodies: Columns "a", "b", "c", "d", and "e" are corresponding to results of 7G7, pVHHS1, 5S1R, VHHS1, and S1R, respectively (Niu et al., 2011). All of the five ricin antibodies were immobilized and reacted with blocking buffer (row 1), ricin (row 2) or abrin (row 3). (B) LOD values for five ricin antibodies (Niu et al., 2011).

VHHS1, and S1R are 5 ng/mL, 500 ng/mL, 1 ng/mL, 1 μg/mL, and 10 ng/mL, respectively (Fig. 3B), which essentially agrees with enzyme-linked immunosorbent assay (ELISA) results. Having the lowest LOD value, 5S1R is considered the best ricin antibody, which may play potential roles in clinical diagnosis and therapy.

Detection of disease biomarkers

Biomarker detection is a powerful method to examine the status of patient tissue and to predict clinical outcomes. BIEs have been applied in this field and demonstrated some success.

Niu et al. (2008) developed a BIE protocol for quantitative measurement of CD146 for tumor marker detection. The CD146 glycoprotein, which may be involved in tumor angiogenesis in endothelial cells, was originally identified as a tumor marker for melanoma. First, CD146 antibody was immobilized by absorption to a protein G-modified silicon substrate. Then, a calibration curve was established for quantitative CD146 detection, and the relationship between the BIE signal y (grayscale value) and the CD146 concentration x (ng/mL) was established ($y = 3.3\ln(x) + 91.3$, as shown in Fig. 4). Finally, 18 serum samples were analyzed to quantify their CD146 concentrations, with detection sensitivity on the order of ng/mL. The majority of these results significantly statistically agree with those of ELISA measurements (Fig. 4C).

Qi et al. (2009b) analyzed 169 patient serum samples by BIE for clinical diagnosis of hepatitis B virus (HBV) infection. Five markers of HBV, including hepatitis B surface antigen (HBsAg), hepatitis B surface antibody (HBsAb), hepatitis B e antigen (HBeAg), hepatitis B e antibody (HBeAb), and

hepatitis B core antibody (HBcAb), are generally used as clinical markers to detect HBV infection. BIE simultaneously detects five markers in eight samples in the same microarray in only 1 h, whereas ELISA can only detect one marker on each plate over a longer time (ligand immobilization and assaying lasts 1–2 days). Moreover, the BIE results are in good agreement with the ELISA results. Sensitivities of 1 ng/mL and 1 IU/mL for HBsAg and HBsAb detection, respectively, have been achieved. The cutoffs (CoVs, i.e., the percentage over the values of the corresponding to negative control produced by national reference negative samples) derived from the receiver operating characteristic (ROC) curves of the five markers (HBsAg, HBsAb, HBeAg, HBeAb, and HBcAb) were deduced to be 15%, 18%, 15%, 20%, and 15%, respectively.

Anastasiadou et al. (2008) evaluated the potential of polarimetric imaging for the early detection and therapy of cervical cancer. The current strategy for cervical cancer detection and therapy is based on detailed examination via a colposcopy. Although being well established, a colposcopy is a very difficult and operator-dependent method, which may lead to a significant proportion of false diagnoses. To develop an additional clinical method, the authors performed the simple linear degree of polarization technique on cone biopsy specimens and found some preliminary but quite encouraging results. A clinical trial of this device is ongoing to compare this imaging modality with classical colposcopy for visualizing cervical precancerous or cancerous lesions.

Jin et al. designed a tumor marker spectrum composed of alpha-fetoprotein (AFP), alpha-L-fucosidase (AFU), and ferritin as a trial to explore its feasibility for the clinical detection of liver cancer, the most prevalent cancer in China, to increase diagnostic specificity (Jin et al., 2011). AFP and
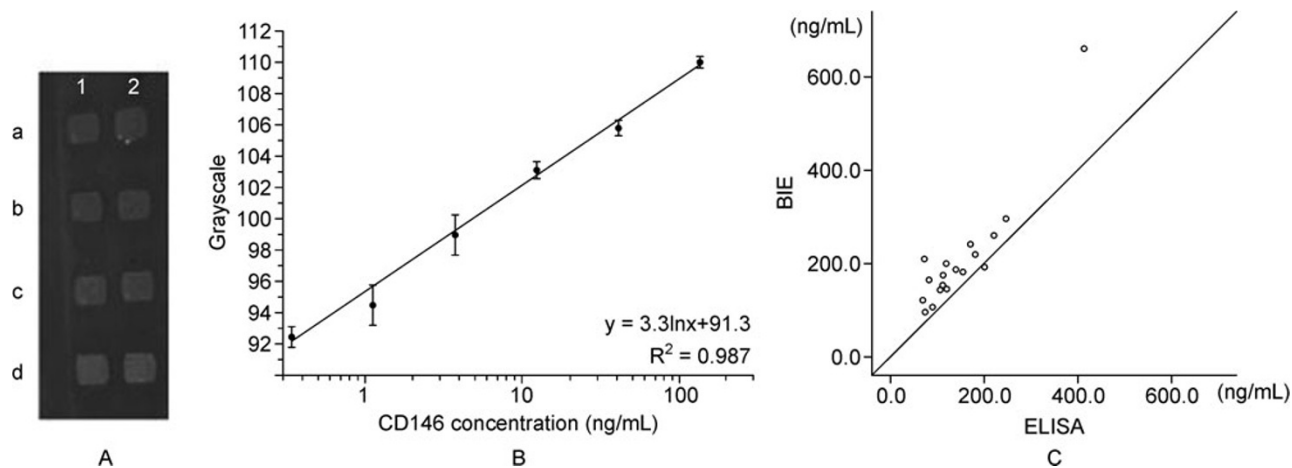
Figure 4. CD146 detection with BIE. (A) CD146 detection: Protein G was immobilized in all of the 8 units. BSA reacts in rows "a" and "b", while CD146 antibody reacts in rows "c" and "d". After blocked by the blocking buffer, one concentration of the CD146 standard sample was added to rows "b" and "d", while PBST was added to rows "a" and "c". In that case, rows "a" and "b" were blank controls, whereas row "c" was negative control (Niu et al., 2008). (B) Calibration curve for quantitative CD146 detection (Niu et al., 2008). (C) Comparison between BIE and ELISA detection results of CD146 from sera of 18 patients: The BIE and ELISA detection results are plotted. A Pearson correlation coefficient of 0.923 indicates that the results of the two methods are significantly correlated at the level of 0.05 (Niu et al., 2008).

AFU are considered novel markers for liver cancer, while ferritin is a marker of many types of cancer. Quantitative detection of AFP, AFU and ferritin are achieved by calibration against standards. The calibration curves of AFP, AFU and ferritin are $y = 13.4 \lg(x) + 79.7$ (detection range from 1 to 64 ng/mL), $y = 24.6 \lg(x) + 88.1$ (detection range from 1 to 64 U/L), and $y = 14.5 \lg(x) + 76.8$ (detection range from 5 to 160 ng/mL), respectively. Here, y is the BIE signal (in grayscale value) and x is the marker concentration (in ng/mL or U/L). The concentrations of AFP, AFU, and ferritin in 56 serum samples composed of 32 normal and 24 liver cancer patients were measured (shown in Fig. 5A), and the results were compared to those obtained by routine clinical approaches, such as enhanced chemiluminescence immunoassay (ECLIA) for AFP, ELISA for AFU, and immunoturbidimetry for ferritin. The Pearson's correlation coefficients of the comparisons are 0.532, 0.948, and 0.937 for AFP, AFU, and ferritin, respectively, which indicates that the results obtained by BIE and routine approaches are significantly statistically similar. ROC curves for single marker detection and logistic regression for joint marker tests were introduced to evaluate BIE's performance in the diagnosis of liver cancer. The area under the curve (AUC), which provides the relationship between the sensitivity and specificity for an independent test, is 0.827, 0.782, and 0.380 for AFP, AFU, and ferritin, respectively (shown in Fig. 5B). However, the AUC increases to 0.884 for joint detection of AFP and AFU, while ferritin is much less related to these two markers. This indicates that the joint detection of tumor markers AFP and AFU may be more useful than their individual detection for clinical liver cancer diagnosis.

Detection of bacterial pathogens

Bacteria are one of the greatest dangers to human health and can cause a series of diseases. Bae et al. (2004) developed an immunosensor with imaging ellipsometry for the purpose of monitoring bacterial pathogens (Bae et al., 2004; Choi and Oh, 2008). *Yersinia enterocolitica* was selected as a typical bacterial pathogen in their study. To fabricate the immunosensor, protein G spots were placed on a gold surface modified by 11-mercaptoundecanoic acid (11-MUA), and then monoclonal antibody was adsorbed onto the protein G spots. The ellipsometric image of the protein G spot and the antibody-adsorbed protein G spot are then obtained. The change in the mean optical intensity of the protein G spot to the various concentrations of *Y. enterocolitica* is shown in Fig. 6. The immunosensor using imaging ellipsometry successfully detected *Y. enterocolitica* at concentrations ranging from 10^3 to 10^7 cfu/mL.

Detection of viruses

Phage M13KO7 is a virus that infects *Escherichia coli*. Because its size and structure is similar to viruses that infect humans, phage M13KO7 is used as a model to develop BIE for direct viral detection. Qi et al. (2009a) directly detected different phage M13KO7 samples, such as natural and purified samples and different batches of samples with various concentrations, with BIE. Their results in Fig. 7A demonstrate that phage M13KO7 can be specifically captured by the ligand when an M13KO7 solution passes over the surface, resulting in a significant increase in the thickness
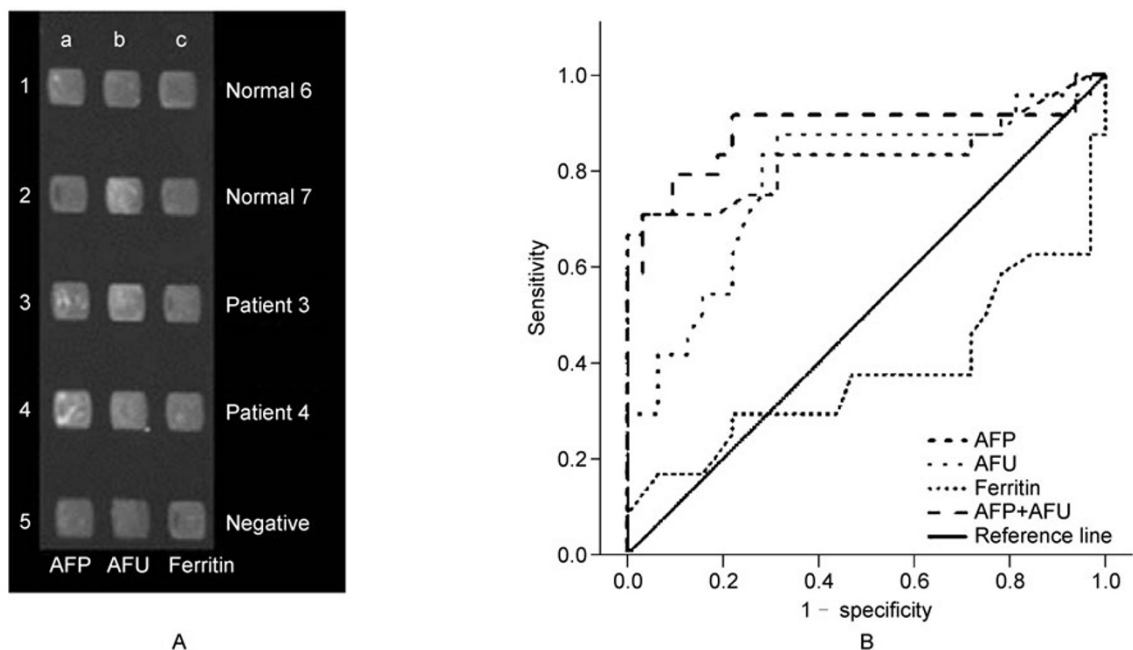
Figure 5.   BIE detection of tumor markers AFP, AFU, and ferritin. (A) Joint detection of AFP, AFU, and ferritin: Columns "a", "b", and "c" were immobilized with anti-AFP, anti-AFU, and anti-ferritin as ligands, respectively. Rows "1", "2", "3", "4", and "5" were reacted with 2 normal sera, 2 patient sera and negative control, respectively (Jin et al., 2011). (B) ROC curve analysis (Jin et al., 2011).
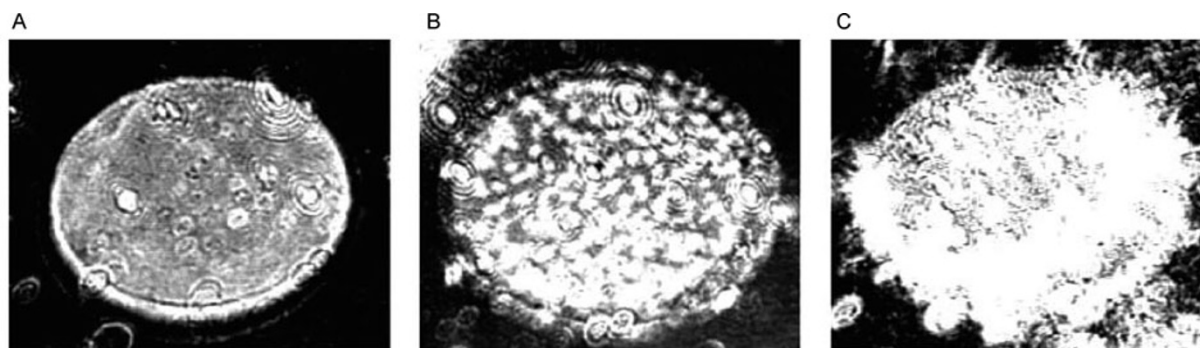
Figure 6.   Ellipsometric images (BIE) of protein G spots bound with various concentrations of *Y. enterocolitica*. (A) 0 cfu/mL, (B) 10^5 cfu/mL, and (C) 10^7 cfu/mL (Bae et al., 2004).

of the anti-M13KO7 binding layer. The detection limit for phage M13KO7 is 10^9 pfu/mL. AFM was also used to confirm that phage M13KO7 was directly captured by ligands on the surface (Fig. 7B). This indicates that BIE is competent for direct detection of phage M13KO7 and has potential in the field of human virus detection.

Avian influenza virus (AIV) has caused global concern as a potential pandemic threat to human life. Qi et al. (2010) used BIE for rapid AIV detection. A sensing surface with multiple antibodies against AIV in a patterned array was constructed as a probe to capture AIV by specific affinity between the antibodies and virus (Fig. 8A). The H5N1 AIV subtype (highly pathogenic) was detected with a sensitivity of 2.56×10^{-3} TCID/mL, which was confirmed by scanning near-field optical microscopy performed in a shear force mode (the image of AIV captured on the sensing surface is shown in Fig. 8B).

BTIRIE EXPERIMENTAL SETUP AND DETECTION PRINCIPLE

In a BTIRIE system, the internal reflection illumination is realized by a coupling prism contacting the glass slide of a micro-fluidic reactor array (Chen et al., 2007b). The other side of the slide is coated with a thin gold film as a substrate for
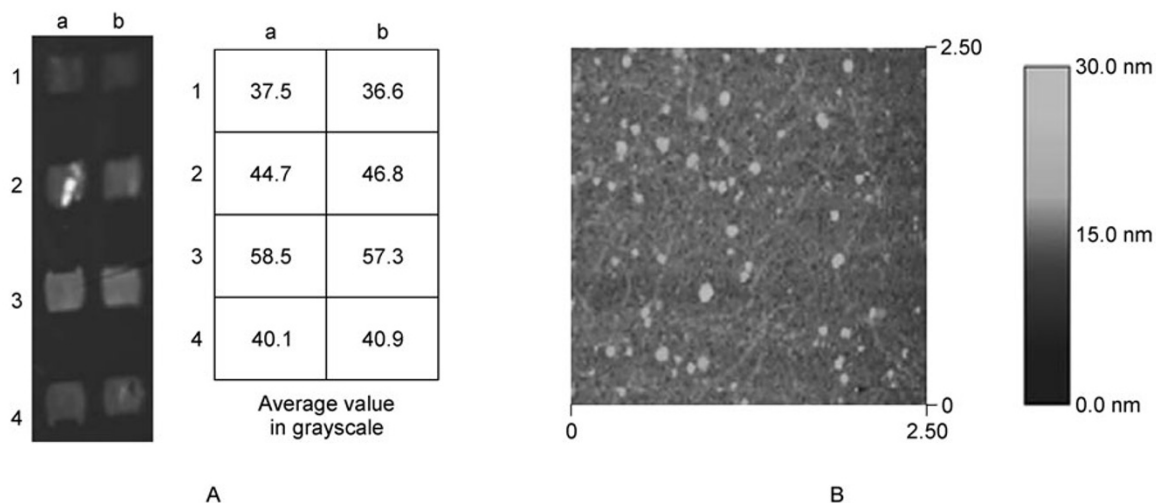
Figure 7. BIE detection of phage M13KO7. (A) A grayscale image verifies specific interaction between bio-GP3 and phage M13KO7: Avidin was first immobilized on all areas, followed by immobilization of bio-GP3 onto areas "a2", "a3", "a4", "b2", "b3", and "b4". PBST was added to areas "a2" and "b2" as control; areas "a3", "b3" and "a4", "b4" were used to detect phage M13KO7 and negative sample (SARS), respectively (Qi et al., 2009a). (B) An AFM image taken from 2.5 μm scanning distance on top of the phage detection area: The overall configuration of phage M13KO7 on the mica surface is presented. The round particles in the image are contaminants in the culture solution, while the phage M13KO7 shows as a long filament with a length of ~ 1 μm, a height of ~ 4 nm and a width of ~ 40 nm (Qi et al., 2009a).
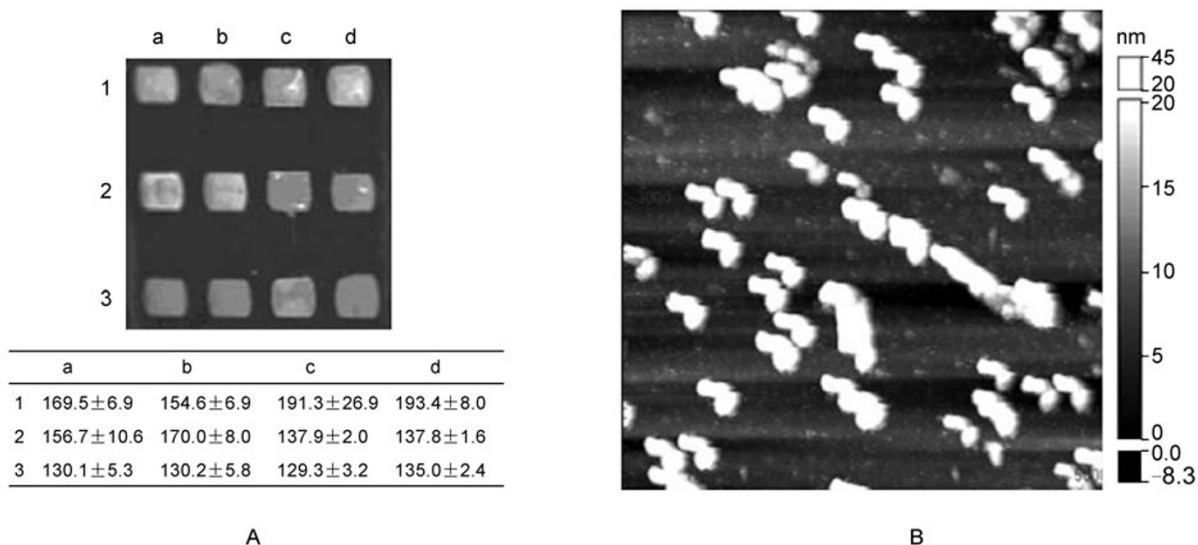
Figure 8. BIE detection of AIV samples. (A) A grayscale image of AIV detection: Antibody ScFv was bound on columns "a" and "b"; antibody 4A4 in ascites was bound on columns "c" and "d". H5N1 was detected in row "1"; H9N2 was detected in row "2"; and row "3" was used as a ligand control (Qi et al., 2010). (B) An image of SNOM in a shear force mode for H5N1 detection (Qi et al., 2010).

ligand immobilization. The probe beam passes through a polarizer and compensator perpendicularly into the window of glass prism and finally onto the gold film (Fig. 9).The incident angle of BTIRIE is fixed and is larger than the critical angle of total internal reflection so that the evanescent wave appearing between the interface of the substrate and the tested solution is used to specifically illuminate the biomolecular interaction in the micro-fluidic reactor array (Chen et al., 2007b). While the evanescent wave field passes the biomolecular layers on the interaction surface, the polarization state of the reflection is modified. Thus, BTIRIE is used to automatically detect label-free protein interactions
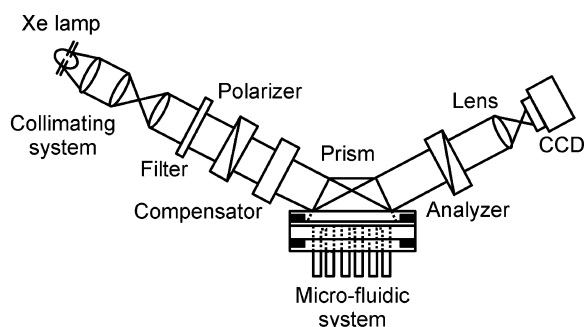
Figure 9. Schematic diagram of the total internal reflection imaging ellipsometry biosensor (BTIRE). The light from a Xe lamp was guided by an optical fiber and expanded by the collimating system. After passing the polarizer and compensator, the polarized collimated beam propagated perpendicularly to the prism and onto the sensing surface. The gold sensing surface was immobilized with ligand for biomolecule interaction in the contacting micro-fluidic reactor array. When the incident angle was larger than the critical angle, the evanescent wave appeared sharply at the sensing surface to detect biomolecule interaction in very shallow depth from the surface. The reflected light carrying surface information was then imaged by CCD camera after passing the analyzer (Chen et al., 2007b).

in real-time. The information of these biomolecular layers are deduced by analysis of the polarized state of the reflection. Further, the shallow illumination depth of the evanescent wave field makes measurements less disturbed by refractive index mismatch, non-uniformity, and flow in the test solution.

BTIRIE APPLICATIONS

In situ BTIRIE is a powerful tool for detecting interactions between biomolecules having weak affinity, with high sensitivity in real-time. A comparison of the real-time detection sensitivity of CD146 was made between the BIE and BTIRIE techniques.

Under the same experimental condition in the BIE measurements (Niu et al., 2008), Liu et al. (2009) applied BTIRIE to quantitatively detect various concentrations (0.1–100 ng/mL) of CD146 (Fig. 10). Although at the lowest concentration of 0.1 ng/mL, the BTIRIE signal is still significantly higher than the reference. This implies that the detection sensitivity of BTIRIE reaches the order of 0.1 ng/mL, which is > 10 times more sensitive than BIE.

Mustafa et al. (2010) exploited spectroscopic BTIRE as a highly sensitive method to detect β-amyloid peptide (Aβ-16). Monoclonal DE2 antibodies were electrostatically immobilized on a gold surface to capture Aβ-16 over a wide range of concentrations. The results demonstrate that interaction between DE2 monoclonal antibodies and Aβ-16 was highly
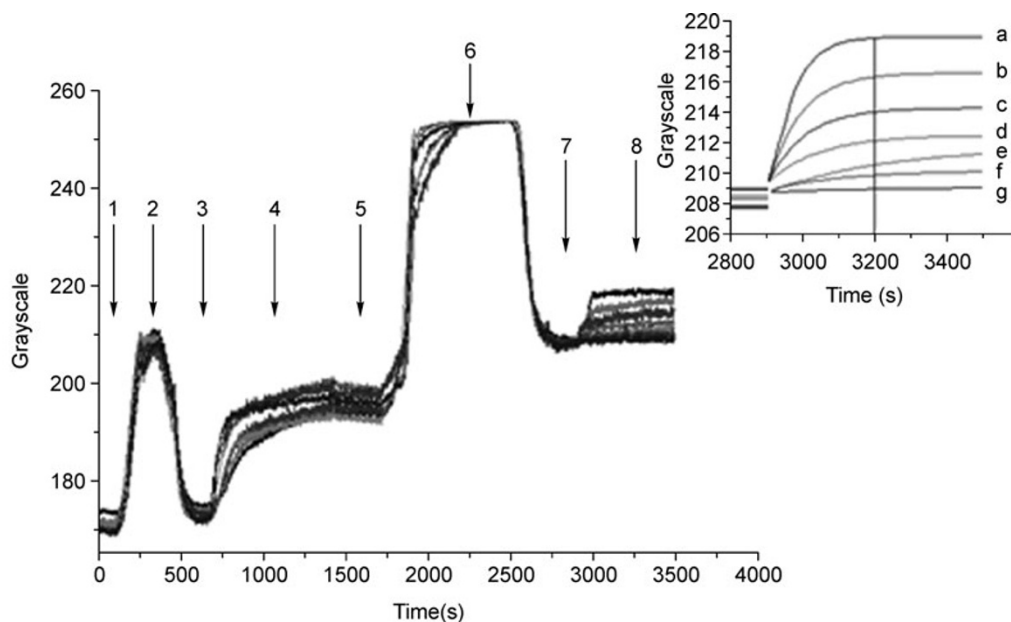
Figure 10. Real-time recording of the dynamic process of CD146 binding with its antibody at various concentrations. Baseline reading was first recorded (region 1), followed by NHS-EDC activation of carboxyl group assembling on the gold substrate (region 2), PBS rising (region 3), CD146 antibody immobilization (region 4), PBS rinsing (region 5), blocking (region 6), PBS rinsing (region 7), and CD146 binding (region 8). Curves "a"–"g" correspond to CD146 concentrations of 100, 40, 20, 10, 1, 0.1, and 0 ng/mL, respectively (Liu et al., 2009).
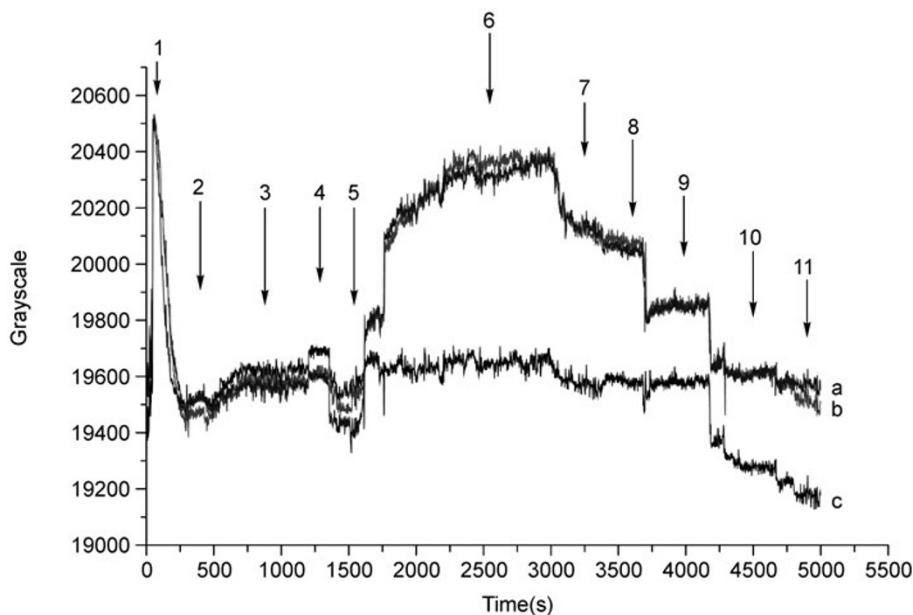
Figure 11.   Real-time recording of the dynamic process of vesicle absorption and release from the surface (Jin et al., 2011). Recording of NHS-EDC activation of carboxyl group assembling on gold substrate (region 1), followed by pure water rising (region 2), 1:100 poly-L-lysine immobilization (region 3), pure water rinsing (region 4), pH 10 glucose solution rinsing (region 5), incubation of vesicles in pH 10 glucose solution, binding to the poly-L-lysine surface (region 6), and flux of pH 10 glucose solution at increasing flow rates (5, 10, 30, 40, and 45 µL/min in regions 7 to 11, respectively).

specific, with an affinity constant $K_D = 1.46×10^{-8}$ mol/L, and the BTIRE detection sensitivity was as low as 0.05 ng/mL.

Vesicle absorption is used to study cell membrane properties due to their similar lipid bilayer structures. Liu et al. applied BTIRIE to visualize the non-specific absorption and release process of vesicles (made of 1,2-Dioleoyl-sn-glycero-3-phosphocholine) from a poly-L-lysine-modified gold surface (Fig. 11; Jin et al., 2011). Region 6 of curves "a" and "b" in Fig. 11 corresponds to the non-specific absorption of vesicles onto the poly-L-lysine surface. In region 7, the glucose solution was changed at a 5 µL/min flux. The corresponding signal decrease indicates vesicles being rinsed off by the glucose solution. When the flux increased to 10 µL/min (region 8), the signal remained nearly the same because the flux was not large enough to remove more vesicles. By increasing the flux to 30 µL/min (region 9), the signal in curves "a" and "b" further decreased but remained constant in reference curve "c". These results demonstrate that vesicles were removed from the surface by the shear-force of the glucose flux, by destroying the non-specific adsorption between vesicles and poly-L-lysine. By increasing the flux to 40 µL/min, the signal in curves "a", "b", and "c" decreased simultaneously, indicating that the poly-L-lysine was also removed from the surface. These results were verified in a parallel experiment performed with a phase contrast microscope (NIKON, TI-U, Japan), indicating that the process of vesicle absorption, release, and poly-L-lysine layer destruction on the surface can be visualized by BTIRIE.

CONCLUSIONS AND PROSPECTIVE

Over the last 16 years, biosensors based on imaging ellipsometry (BIEs and BTIREs) have been developed as label-free, high-throughput, and automated techniques for protein detection in a simple operation. The successful experiments described above prove that these techniques are suitable tools for biomedical and clinical applications. Aside from having the same advantages of being label-free, non-contact, and ultra-highly sensitive, BTIRIE excels over BIE by avoiding errors in the *ex situ* mode. Having high potential to monitor weak and transient biological interactions in real-time, which is very difficult for traditional approaches, BTIRIE has become a powerful technique for biomolecular detection as well as in clinical diagnosis.

ACKNOWLEDGEMENTS

ABBREVIATIONS

AIV, avian influenza virus; BIEs, biosensors based on imaging ellipsometry; BTIRIEs, biosensors based on total internal reflection imaging ellipsometry; ECLIA, enhanced chemiluminescence immu-

noassay; HBV, hepatitis B virus; LOD, limit of detection; SIE, spectroscopic imaging ellipsometry; SPR, surface plasmon resonance; SPRi, SPR imaging

REFERENCES

Aicher, A., Brenner, W., Zuhayra, M., Badorff, C., Massoudi, S., Assmus, B., Eckey, T., Henze, E., Zeiher, A.M., and Dimmeler, S. (2003). Assessment of the tissue distribution of transplanted human endothelial progenitor cells by radioactive labeling. Circulation 107, 2134–2139.

Anastasiadou, M., Martino, A.D., Clement, D., Liège, F., Laude-Boulesteix, B., Quang, N., Dreyfuss, J., Huynh, B., Nazac, A., Schwartz, L., *et al.* (2008). Polarimetric imaging for the diagnosis of cervical cancer. Physica Status Solidi (c) 5, 1423–1426.

Arwin, H. (1998). Spectroscopic ellipsometry and biology: recent developments and challenges. Thin Solid Films 313, 764–774.

Asinovski, L., Beaglehole, D., and Clarkson, M.T. (2008). Imaging ellipsometry: quantitative analysis. Physica Status Solidi a-Applications and Materials Science 205, 764–771.

Bae, Y.M., Oh, B.K., Lee, W., Lee, W.H., and Choi, J.W. (2004). Immunosensor for detection of Yersinia enterocolitica based on imaging ellipsometry. Anal Chem 76, 1799–1803.

Bally, M., Halter, M., Voros, J., and Grandin, H.M. (2006). Optical microarray biosensing techniques. Surf Interface Anal 38, 1442–1458.

Boozer, C., Kim, G., Cong, S.X., Guan, H.W., and Londergan, T. (2006). Looking towards label-free biomolecular interaction analysis in a high-throughput format: a review of new surface plasmon resonance technologies. Curr Opin Biotechnol 17, 400–405.

Campbell, C.T., and Kim, G. (2007). SPR microscopy and its applications to high-throughput analyses of biomolecular binding events and their kinetics. Biomaterials 28, 2380–2392.

Chan, W.C.W., and Nie, S.M. (1998). Quantum dot bioconjugates for ultrasensitive nonisotopic detection. Science 281, 2016–2018.

Chen, Y.Y., Meng, Y.H., and Jin, G. (2007a). Optimization of off-null ellipsometry for air/solid interfaces. Appl Opt 46, 8475–8481.

Chen, Y.Y., Wang, Z.H., Meng, Y.H., and Jin, G. (2007b). Biosensor with total internal reflection imaging ellipsometry. International Journal of Nanotechnology 4, 171–178.

Choi, J.W., and Oh, B.K. (2008). Optical Detection of Pathogens using Protein Chip. In: Advanced Environmental Monitoring. Y. J. Kim, and U. Platt, eds. Springer Netherlands. 348–362.

Cornell, B.A., Braach-Maksvytis, V.L., King, L.G., Osman, P.D., Raguse, B., Wieczorek, L., and Pace, R.J. (1997). A biosensor that uses ion-channel switches. Nature 387, 580–583.

Engvall, E., and Perlmann, P. (1971). Enzyme-linked immunosorbent assay (ELISA). Quantitative assay of immunoglobulin G. Immunochemistry 8, 871–874.

Gedig, M., Faiss, S., and Janshoff, A. (2008). Melting and interdigitation of microstructured solid supported membranes quantified by imaging ellipsometry. Biointerphases 3, FA51–FA58.

Huang, C., Chen, Y., and Jin, G. (2011). A one-step immunoassay for carbohydrate antigen 19-9 by biosensor based on imaging ellipsometry. Ann Biomed Eng 39, 185–192.

Hutter, E., and Fendler, J.H. (2004). Exploitation of localized surface plasmon resonance. Adv Mater (Deerfield Beach Fla) 16, 1685–1706.

Jain, P.K., Huang, X., El-Sayed, I.H., and El-Sayed, M.A. (2007). Review of some interesting surface plasmon resonance-enhanced properties of noble metal nanoparticles and their applications to biosystems. Plasmonics 2, 107–118.

Jin, G. (2008). Development of biosensor based on imaging ellipsometry. Physica Status Solidi a-Applications and Materials Science 205, 810–816.

Jin, G., Jansson, R., and Arwin, H. (1996). Imaging ellipsometry revisited: Developments for visualization of thin transparent layers on silicon substrates. Rev Sci Instrum 67, 2930–2936.

Jin, G., Meng, Y.H., Liu, L., Niu, Y., Chen, S., Cai, Q., and Jiang, T.J. (2011). Development of biosensor based on imaging ellipsometry and biomedical applications. Thin Solid Films 519, 2750–2757.

Jin, G., Tengvall, P., Lundström, I., and Arwin, H. (1995). A biosensor concept based on imaging ellipsometry for visualization of biomolecular interactions. Anal Biochem 232, 69–72.

Jin, G., and Wang, Z.H. (2002). Micro-systems for optical protein-chip. International Journal of Nonlinear Sciences and Numerical Simulation 3, 191–194.

Klenkar, G., and Liedberg, B. (2008). A microarray chip for label-free detection of narcotics. Anal Bioanal Chem 391, 1679–1688.

Kodadek, T. (2001). Protein microarrays: prospects and problems. Chem Biol 8, 105–115.

Kodoyianni, V. (2011). Label-free analysis of biomolecular interactions using SPR imaging. Biotechniques 50, 32–40.

Ladbury, J.E., and Chowdhry, B.Z. (1996). Sensing the heat: the application of isothermal titration calorimetry to thermodynamic studies of biomolecular interactions. Chem Biol 3, 791–801.

Ligler, F.S., Taitt, C.R., Shriver-Lake, L.C., Sapsford, K.E., Shubin, Y., and Golden, J.P. (2003). Array biosensor for detection of toxins. Anal Bioanal Chem 377, 469–477.

Liu, L., Chen, Y.Y., Meng, Y.H., Chen, S., and Jin, G. (2011). Improvement for sensitivity of biosensor with total internal reflection imaging ellipsometry (TIRIE). Thin Solid Films 519, 2758–2762.

Liu, L., Niu, Y., Chen, S., Meng, Y., Ma, H., and Jin, G. (2010). Optimization of evanescent wave imaging for the visualization of protein adsorption layers. Science China: Physics. Mechanics and Astronomy 53, 1805–1810.

Liu, L., Niu, Y., Meng, Y., Chen, S., Yan, X., and Jin, G. (2009). CD146 detection with real-time total internal reflection imaging ellipsometry. Paper presented at: World Congress on Medical Physics and Biomedical Engineering: Micro- and Nanosystems in Medicine, Active Implants, Biosensors, Sept 7–12, 2009. Munich, Germany: Springer-Verlag.

Lucklum, R., and Hauptmann, P. (2000). The quartz crystal microbalance: mass sensitivity, viscoelasticity and acoustic amplification. Sens Actuators B Chem 70, 30–36.

Meng, Y.H., and Jin, G. (2011). Rotating compensator sampling for spectroscopic imaging ellipsometry. Thin Solid Films 519, 2742–2745.

Mustafa, M.K., Nabok, A., Parkinson, D., Tothill, I.E., Salam, F., and Tsargorodskaya, A. (2010). Detection of β-amyloid peptide (1-16) and amyloid precursor protein (APP770) using spectroscopic ellipsometry and QCM techniques: a step forward towards Alzheimers disease diagnostics. Biosens Bioelectron 26, 1332–1336.

Niu, Y., Zhang, Y., Yan, X., and Jin, G. (2008). Approach to

quantitative detection of CD146 with a label-free protein biosensor based on imaging ellipsometry. Paper presented at: 4th European Conference of the International Federation for Medical and Biological Engineering, ECIFMBE 2008, November 23–27, 2008. Antwerp, Belgium: Springer-Verlag.

Niu, Y., Zhuang, J., Liu, L., Yan, X., and Jin, G. (2011). Two kinds of anti-ricin antibody and ricin interaction evaluated by biosensor based on imaging ellipsometry. Thin Solid Films 519, 2768–2771.

Qi, C., Lin, Y., Feng, J., Wang, Z.H., Zhu, C.F., Meng, Y.H., Yan, X.Y., Wan, L.J., and Jin, G. (2009a). Phage M13KO7 detection with biosensor based on imaging ellipsometry and AFM microscopic confirmation. Virus Res 140, 79–84.

Qi, C., Tian, X.S., Chen, S., Yan, J.H., Cao, Z., Tian, K.G., Gao, G.F., and Jin, G. (2010). Detection of avian influenza virus subtype H5 using a biosensor based on imaging ellipsometry. Biosens Bioelectron 25, 1530–1534.

Qi, C., Zhu, W., Niu, Y., Zhang, H.G., Zhu, G.Y., Meng, Y.H., Chen, S., and Jin, G. (2009b). Detection of hepatitis B virus markers using a biosensor based on imaging ellipsometry. J Viral Hepat 16, 822–832.

Rich, R.L., and Myszka, D.G. (2007). Higher-throughput, label-free, real-time molecular interaction analysis. Anal Biochem 361, 1–6.

Scarano, S., Mascini, M., Turner, A.P.F., and Minunni, M. (2010). Surface plasmon resonance imaging for affinity-based biosensors.

Biosens Bioelectron 25, 957–966.

Templin, M.F., Stoll, D., Schwenk, J.M., Pötz, O., Kramer, S., and Joos, T.O. (2003). Protein microarrays: promising tools for proteomic research. Proteomics 3, 2155–2166.

Wanekaya, A.K., Chen, W., Myung, N.V., and Mulchandani, A. (2006). Nanowire-based electrochemical biosensors. Electroanalysis 18, 533–550.

Wang, Z.H., and Jin, G. (2003a). Feasibility of protein A for the oriented immobilization of immunoglobulin on silicon surface for a biosensor with imaging ellipsometry. J Biochem Biophys Methods 57, 203–211.

Wang, Z.H., and Jin, G. (2003b). A label-free multisensing immuno-sensor based on imaging ellipsometry. Anal Chem 75, 6119–6123.

Wang, Z.H., and Jin, G. (2004a). Covalent immobilization of proteins for the biosensor based on imaging ellipsometry. J Immunol Methods 285, 237–243.

Wang, Z.H., and Jin, G. (2004b). Silicon surface modification with a mixed silanes layer to immobilize proteins for biosensor with imaging ellipsometry. Colloids Surf B Biointerfaces 34, 173–177.

Wang, Z.H., Meng, Y.H., Ying, P.Q., Qi, C., and Jin, G. (2006). A label-free protein microfluidic array for parallel immunoassays. Electro-phoresis 27, 4078–4085.

Yu, X.B., Xu, D.K., and Cheng, Q. (2006). Label-free detection methods for protein microarrays. Proteomics 6, 5493–5503.